Environmental Pollution 345 (2024) 123460

Contents lists available at ScienceDirect

Environmental Pollution

journal homepage: www.elsevier.com/locate/envpol

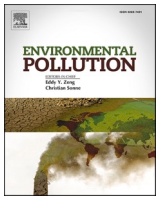

Bioaccumulation and biotransformation of 1,2-bis (2,4,6-tribromophenoxyethane) (BTBPE) and 1,2-dibromo-4-(1,2-dibromoethyl)-cyclohexane (TBECH) in zebrafish (*Danio rerio*)☆

Yu-Yu Wang [1], Wei-Keng Luo [1], Song-Xiong Tang, Jun Xiang, Yao Dang, Bin Tang [*], Qi-Yuan Lu, Feng-Shan Cai, Ming-Zhong Ren, Yun-Jiang Yu, Jing Zheng

State Environmental Protection Key Laboratory of Environmental Pollution Health Risk Assessment, Research Center of Emerging Contaminants, South China Institute of Environmental Sciences, Ministry of Ecology and Environment, Guangzhou, 510530, PR China

ARTICLE INFO

Keywords:
1,2-Bis (2,4,6-tribromophenoxyethane) (BTBPE)
1,2-Dibromo-4-(1,2-dibromoethyl)-cyclohexane (TBECH)
Zebrafish
Tissue-specific accumulation
Transformation products

ABSTRACT

Despite the increasing production, use, and ubiquitous occurrence of novel brominated flame retardants (NBFRs), little information is available regarding their fate in aquatic organisms. In this study, the bioaccumulation and biotransformation of two typical NBFRs, i.e., 1,2-bis (2,4,6-tribromophenoxyethane) (BTBPE) and 1,2-dibromo-4-(1,2-dibromoethyl)-cyclohexane (TBECH), were investigated in tissues of zebrafish (*Danio rerio*) being administrated a dose of target chemicals through their diet. Linear accumulation was observed for both BTBPE and TBECH in the muscle, liver, gonads, and brain of zebrafish, and the elimination of BTBPE and TBECH in all tissues followed pseudo-first-order kinetics, with the fastest depuration rate occurring in the liver. BTBPE and TBECH showed low bioaccumulation potential in zebrafish, with biomagnification factors (BMFs) < 1 in all tissues. Individual tissues' function and lipid content are vital factors affecting the distribution of BTBPE and TBECH. Stereoselective accumulation of TBECH enantiomers was observed in zebrafish tissues, with first-eluting enantiomers, i.e. E_1-α-TBECH and E_1-β-TBECH, preferentially accumulated. Additionally, the transformation products (TPs) in the zebrafish liver were comprehensively screened and identified using high-resolution mass spectrometry. Twelve TPs of BTBPE and eight TPs of TBECH were identified: biotransformation pathways involving ether cleavage, debromination, hydroxylation, and methoxylation reactions for BTBPE and hydroxylation, debromination, and oxidation processes for TBECH. Biotransformation is also a vital factor affecting the bioaccumulation potential of these two NBFRs, and the environmental impacts of NBFR TPs should be further investigated in future studies. The findings of this study provide a scientific basis for an accurate assessment of the ecological and environmental risks of BTBPE and TBECH.

1. Introduction

Brominated flame retardants (BFRs) have been extensively utilized as additives to enhance the fire resistance of plastics, textiles, rubber, electronics, clothing, and construction materials (Cao et al., 2018; Hou et al., 2021; Xiong et al., 2019). The recently strict regulations imposed on the use of legacy BFRs like polybrominated diphenyl ethers (PBDEs) and hexabromocyclododecanes (HBCDs) led to the utilization of several "novel" BFRs (NBFRs) as alternatives to meet flammability standards (Wang et al., 2023; Xiong et al., 2019). The global production of NBFRs is estimated to be 100–180 kt per year, of which 1,2-bis (2,4,6-tribromophenoxy) ethane (BTBPE) and 1,2-dibromo-4-(1,2-dibromoethyl) cyclohexane (TBECH) are the main substitutes for the Octa- and Penta-BDE technique mixtures (Hou et al., 2021; McGrath et al., 2017; Xiong et al., 2019; Zuiderveen et al., 2020). Specifically, TBECH has four diastereomeric pairs of enantiomers, with generally equal amounts of α- and β-TBECH, and minor content of γ- and δ-TBECH as impurities in the technical formulation (Ruan et al., 2018b). Because NBFRs are not chemically bound to products, they can be easily released into the environmental matrices, including air, dust, water, and sediment, during

☆ This paper has been recommended for acceptance by Charles Wong.

* Corresponding author.
E-mail address: tangbin@scies.org (B. Tang).

[1] These authors contributed equally to this work.

https://doi.org/10.1016/j.envpol.2024.123460
Received 17 November 2023; Received in revised form 22 January 2024; Accepted 26 January 2024
Available online 28 January 2024

their production, application, and disposal processes (Li et al., 2019; Wang et al., 2019; Wang et al., 2023; Xiong et al., 2019). To date, BTBPE and TBECH have been ubiquitously detected in the environment and biotas, and have been identified to have long-range transportation and potential toxicity, which deserve more attention concerning their environmental risks (Bu et al., 2019; Hou et al., 2021; Ling et al., 2021; Marteinson et al., 2017; Shi et al., 2021; Stojak et al., 2019).

Characterization of the bioaccumulation properties of NBFRs is vital for assessing their ecological risks (Hou et al., 2022; Wang et al., 2019; Wang et al., 2023; Zheng et al., 2018). Because of the high lipophilicity of BTBPE (log Kow = 7.88) and TBECH (log Kow = 5.24), they are potentially bioaccumulative in aquatic biota. However, the bioaccumulation of BTBPE and TBECH varies in both freshwater and marine environments. The calculated bioaccumulation factors (BAFs) for α-TBECH, β-TBECH, and BTBPE were 400–9800 L/kg (mean 2000 L/kg), 250–10000 L/kg (mean 2600 L/kg), 630–15000 L/kg (mean 4700 L/kg), respectively, in crucian carp (*Carassius auratus*) collected from an electronic waste recycling area in China; although the mean BAFs values of these three chemicals were less than 5000, their potential of bioaccumulation should not be neglected (Wang et al., 2023). BTBPE and TBECH showed magnification potential in marine food webs in the Bohai Sea and the South China Sea (Hou et al., 2022; Liu et al., 2021). Trophic magnification was observed for BTBPE, whereas β-TBECH showed trophic dilution in the food web of Taihu Lake (Zheng et al., 2018). Trophic dilution has also been observed for BTBPE in the aquatic food chain of Lake Ontario (Kurt-Karakus et al., 2019). However, the underlying causes of bioaccumulation of BTBPE and TBECH in aquatic organisms remain unclear.

In addition to the physicochemical properties, biotransformation *in vivo* is also a vital factor affecting the bioaccumulation potential of NBFRs. However, few studies have investigated the biotransformation of BTBPE and TBECH in aquatic biota. No reductive debromination or hydroxylation of BTBPE was observed in rainbow trout (*Oncorhynchus mykiss*) administrated BTBPE through dietary exposure, and the biomagnification factors (BMFs) of BTBPE were calculated as 2.30 ± 0.90 (Tomy et al., 2007). 2, 4, 6-tribromophenol (TBP) was identified as the major transformation product (TP) in zebrafish (*Danio rerio*) (Qiao et al., 2023) and fathead minnow (*Pimephales promelas*) (de Jourdan et al., 2014). Monohydroxy-TBECH was identified as the primary TP of TBECH in human and rat liver microsomal assays (Chu et al., 2012; Nguyen et al., 2017). However, the biotransformation pathways of BTBPE and TBECH in aquatic biota are still poorly understood.

A few studies have also reported enantiomer-specific accumulation of TBECH in biota. Marine biotas show significant enantioselective accumulation of α-, γ-, and δ-TBECH enantiomeric pairs, while no such accumulation was observed for β-TBECH (Ruan et al., 2018a; Ruan et al., 2018b). Earthworms were found to enantioselective accumulate E_1-α-TBECH and E_2-γ-TBECH enantioselectively (Yang et al., 2022). These results suggest the enantiomer-selective accumulation or biotransformation of TBECH in biota, as only biologically mediated processes, can change the enantiomeric composition of chiral chemicals (Eljarrat et al., 2008; Huang et al., 2022; Kania-Korwel and Lehmler, 2016; Wong, 2006). However, the metabolites of TBECH were not identified in these studies, and the biotransformation of TBECH requires further investigation.

In the present study, zebrafish specimens (*Danio rerio*) were administered to a dose of BTBPE and α-/β-TBECH through diet for 28 days. Afterwards, the zebrafish underwent a 77-day depuration period where they were fed unfortified food. The major objectives of this study were to (1) examine the uptake and depuration behaviors of BTBPE and α-/β-TBECH in zebrafish tissues, (2) investigate the stereospecific accumulation of α-/β-TBECH, and (3) comprehensively screen and identify the TPs of BTBPE and α-/β-TBECH *in vivo*. The results of this study address the information gap on the bioaccumulation of BTBPE and α-/β-TBECH. Furthermore, it helps to explore the influences of biotransformation in organisms on accumulating these chemicals in aquatic biotas.

2. Materials and methods

2.1. Chemicals and reagents

Standards of α-/β-TBECH mixture, BTBPE, and BDEs 77 and 118 (purity >95 %) were acquired from AccuStandard (New Haven, CT, USA). HPLC-grade dichloromethane (DCM), acetone (ACE), n-hexane (Hex), andethyl acetate (ETAC), and guaranteed reagent-grade anhydrous sodium sulfate and concentrated sulfuric acid (H_2SO_4) were purchased from CNW Technologies GmbH (Dusseldorf, Germany).

2.2. Exposure experiment design

Mixture of α-/β-TBECH (75 μg) and BTBPE (60 μg) were spiked into 5 g of cod liver oil, and thoroughly homogenized with 50 g of commercial fish food pellets. The spiked fish food was stored in the dark at 4 °C throughout exposure experiment. The designing level (1200 ng/g dry weight (dw)) of BTBPE is in accordance with the highest reported concentration of BTBPE (1100 ng/g dw) in sediment from an e-waste site in East China (Ling et al., 2021). The designing total level of α-/β-TBECH was 1500 ng/g dw (750 ng/g dw for α- and β-TBECH, respectively), which was comparable to that of BTBPE in the spiked food. The α-TBECH level was approximately ten times that (73.2 ng/g dw) in sludge in a wastewater treatment plant in Harbin (Li et al., 2018). Non-spiked food was prepared following identical procedures, excluding the addition of target chemicals.

Three hundred zebrafish (*Danio rerio;* wild type, AB strain, four-month-old) were acquired from Institute of Hydrobiology, Chinese Academy of Sciences. The initial weights and lengths of the zebrafish were recorded as 0.65 ± 0.21 g and 4.01 ± 0.16 cm, respectively. Twenty-five background samples were randomly collected, while a control group of fifty-five zebrafish was selected and kept in a glass aquarium. The other 220 zebrafish were kept in four aquariums as the treatment group. The aquariums were maintained with a 12-h/12-h light-dark cycle, using dechlorinated tap water at a temperature of 22–23 °C, pH at 6.5–7.5, and dissolved oxygen at 7.8–8.4 mg/L. Before exposure, the zebrafish were fed non-spiked food for 14 d to acclimatize to their new surroundings. A feeding rate as 1 % of the mean weight of zebrafish per day was maintained.

Following a 28-d exposure period, the exposed group underwent an additional 77-d depuration, during which the zebrafish were fed non-spiked food. The control group was provided with non-spiked food throughout the experiment. Fish sampling was conducted at 0, 7, 14, 21, and 28 d of the uptake period, and at 7, 21, 35, 49, 63, and 77 d of the depuration period. A random selection of 20 zebrafish was collected from each aquarium in the treated group, while five fish were randomly sampled from the control group on each sampling day. The fish were carefully dissected and separated into the liver, gonads, brain, and muscle, and the mass of individual tissues were recorded. A liver aliquot (1/5 of total weight) collected on each sampling day was combined into a single sample for the screening of BTBPE and TBECH TPs. Also, on each sampling day, approximately 0.5 g of spiked food was collected to determine the concentrations of the target chemicals using the analytical procedures described below.

2.3. Sample pretreatment

The fish tissues (muscle, liver, brain, and gonads) and food pellets underwent pretreatment procedures following the methodologies described in previous studies (Peng et al., 2014; Tang et al., 2018), with a minor modification. The sample was freeze-dried, ground into powder, weighed (~0.5 g for zebrafish muscle and food pellets, and 50–200 mg for liver, gonads, and brain of zebrafish), and spiked with internal standard (IS; BDE 118, 20 ng) in a 10-mL glass tube, and ultrasonication

extracted three times with 5 mL Hex/ACE (1:1, v/v). After centrifugation (3500 rpm, 5 min), the supernatant was collected in a precleaned glass tube, concentrated to near dryness, and then reconstituted in Hex (10 mL). The lipid content was quantified using a 2.0 mL aliquot of the reconstituted sample. The remaining extract (~8.0 mL) was treated with H_2SO_4 (3 mL, twice) to eliminate lipids. The lipid-free extract was condensed to ~1 mL and subsequently purified using a Florisil® ENVI cartridge (500 mg, 3 mL) that precleaned with 6 mL ETAC and 6 mL Hex. Ten mL of Hex/DCM (v/v = 1:1) was used to eluate the target chemicals. The eluate was concentrated to near dryness, reconstituted in a mixture of 20 μL recovery standard (BDE 77, 20 ng) and 180 μL isooctane, and was kept at −20 °C prior to instrumental analysis.

Combined liver samples were pretreated for TP screening following the methodology outlined in previous studies (Chen et al., 2019; Wang et al., 2016), with a minor modification. Briefly, the liver sample (50–200 mg) was fortified with the IS (BDE 118, 20 ng), 100 μL MeOH, and 20 μL formic acid into a 2-mL glass tube. The sample was then vortexed (1800 rpm, 5 min) and ultrasonication extracted with 1 mL of MeOH/ACE (1:1, v/v) for three times. After centrifugation (3500 rpm, 5 min), the supernatant was combined, and 50 mg of C_{18} sorbent powder was added to remove fat and impurities from the extract. After being vortexed (800 rpm, 5 min) and centrifuged (8000 rpm, 5 min), the supernatant was collected and concentrated to near dryness, and was then reconstituted in 100 μL MeOH prior to instrumental analysis.

2.4. Instrumental analysis

The quantification of BTBPE and TBECH was conducted by using an Agilent 7890A gas chromatography coupled with an Agilent 5975B mass spectrometry (GC-MS; Agilent Technology, Palo Alto, CA, USA), and electron capture negative ionization (ECNI) source utilized in a selective ion monitoring (SIM) mode was applied (Tang et al., 2021). Separation of target chemicals was achieved by a DB-HT capillary column (15 m × 0.25-mm i.d. × 0.25-μm film thickness, J&W Scientific, Folsom, CA, USA). In addition, the same instrumental method operated in full scan mode was used to screen the potential debrominated TPs of BTBPE and TBECH in the zebrafish livers.

TBECH enantiomers were separated using GC-MS (Agilent 7890A-5975C, Palo Alto, USA) with the electron ionization (EI) source in a SIM mod (Ruan et al., 2018b; Yang et al., 2022). Separation of α-TBECH and β-TBECH enantiomers was performed by using a MEGA-176MS column (15 m × 0.25 mm i.d. × 0.18 μm film thickness, MEGA, Italy) and a CHIRALDEX B-TA capillary column (30 m × 0.25 μm i.d., 0.12 μm film thickness, Supelco, Bellefonte, PA, USA), respectively. Additional information on the GC-MS parameters is provided in details in the Supplementary Material (SM, Text S1).

The possible TPs of BTBPE and TBECH were further screened using an Agilent 1290 Infinity ultra-high performance liquid chromatography coupled with an Agilent 6545 quadrupole time-of-flight mass spectrometer (UPLC-QTOF-MS; Agilent Technology, Santa Clara, CA, USA), electrospray ionization source operating in positive (ESI+) and negative (ESI–) modes was used (Baduel et al., 2019; Chu et al., 2012). UPLC separation was performed on an RRHD Eclipse Plus 95-C_{18} (3 mm × 150 mm, 1.8 μm film thickness; Agilent Technologies, Palo Alto, USA). The detailed instrumental parameters and the identification of TPs were based on the method described in previous studies (Baduel et al., 2019; Chu et al., 2012; Xiong et al., 2020), with details presented in the SM (Text S2).

2.5. Quality assurance and control

Quality assurance and control procedures for quantifying NBFRs involved regular analysis of native spiked blank (n = 6) and matrix samples (n = 6), and procedural blank samples. The IS corrected recoveries of BTBPE, α-TBECH, and β-TBECH in the native spiked blank and matrix samples were calculated for accuracies, which were 87–115 %, 92–109 %, and 88–97 %, respectively, with relative standard deviations (RSDs) below 20 %. Procedural blank samples (n = 10) were performed on each extraction batch to monitor background interference and contamination. Target chemicals were not detected in procedural blanks. The recoveries of BDE 118 in all samples (n = 260) were 88–102 %, further indicated the robustness of the analytical method. The lowest calibration point that produced a signal-to-noise ratio (S/N) of 10 was used to calculate the limits of quantification (LOQs) for the analyte. The LOQs were 0.10–0.22 ng/g lw in fish tissues and 0.08–0.32 ng/g dw in food samples, respectively.

2.6. Statistical analysis

The lipid-corrected bioaccumulation parameters of BTBPE and TBECH in fish tissues (in lipid basis concentrations), as well as the enantiomeric composition of TBECH that quantified in terms of enantiomer fractions (EFs), were calculated using equations previously reported in the literature (Arnot and Quinn, 2015; Harner et al., 2000; OECD, 2012; Tang et al., 2018), which present in details in the SM (Text S3).

Statistical analyses were performed using the SPSS 22 for Windows (NY, IBM Corp., Armonk, USA). The potential statistical differences in the inter-tissue variability of BTBPE and TBECH levels were examined by one-way analysis of variance (ANOVA). The differences between the fish weight and length on different sampling days were assessed by a paired-sample *t*-test. Spearman's correlation analysis was employed to analyze the correlation between the levels of BTBPE and TBECH in wet-weight and the lipid content in tissues. The significance level was set at $p < 0.05$.

3. Results and discussion

3.1. Levels in control groups

No significant difference was observed in the fish weights and lengths, respectively, between the control group (0.69 ± 0.04 g, 4.01 ± 0.18 cm) and the exposed group (0.70 ± 0.06 g, 4.07 ± 0.13 cm), during the 105-day experiment (one-way ANOVA, $p > 0.05$). These values remained relatively stable throughout the experiment duration, exhibiting no significant changes with the initial values (*t*-test, $p > 0.05$). Furthermore, the fish growth rate constant (k_g) was derived by fitting the natural log-transformed zebrafish weights and lengths over the experiment duration, and no significant difference was found between k_g values (the slopes of the fitted curves) and zero in both the control and exposed groups (Fig. S1), indicating the relatively low growth rates for zebrafish. Thus, the effects of growth dilution on the BTBPE and TBECH levels in zebrafish tissues were neglected in this study. In addition, the levels of NBFRs in zebrafish in the control group and non-spiked food were below the LOQs, suggesting that the background interference of BTBPE and TBECH was negligible. The concentrations of BTBPE, α-TBECH, and β-TBECH in the spiked food samples collected throughout the exposure period were 1210 ± 21.5, 735 ± 18.1, and 728 ± 22.3 ng/g dw, respectively, which closely approximated the nominal concentration. Meanwhile, no apparent depletion was found in the levels of target chemicals over the exposure period (Fig. S2), indicating they are stable in the spiked food. The measured BTBPE, α-TBECH, and β-TBECH levels in the spiked food samples were used to calculate the bioaccumulation parameters.

3.2. Bioaccumulation parameters

The bioaccumulation kinetic constants of BTBPE, α-TBECH, and β-TBECH were examined in the muscle, liver, gonads, and brain of zebrafish, as the other tissues (e.g., heart and spleen) were not easy to separate, or the amount of tissue after separation was not sufficient for analysis. After seven days of exposure, BTBPE, α-TBECH, and β-TBECH

were detected in all target tissues (Fig. 1). Similar uptake curves were observed for α-TBECH and β-TBECH in individual tissues, which were slightly different to those for BTBPE (Fig. 1). BTBPE, α-TBECH, and β-TBECH were linearly accumulated in zebrafish tissues during the uptake phase (Fig. 1), with the highest levels attained at the end of uptake period (28 d) (Fig. 1), which did not reach a steady state. An apparent declining trend was observed for BTBPE, α-TBECH, and β-TBECH levels in all tissues in the depuration period, following a pseudo-first-order depuration kinetics (Fig. 1). The bioaccumulation kinetics constants, including assimilation efficiencies (α), depuration rates (kd), depuration half-lives ($t_{1/2}$), and biomagnification factors (BMFs), of BTBPE, α-TBECH, and β-TBECH in zebrafish tissues were calculated (Table 1).

The liver showing the highest α values, followed by the gonad and muscle, with the lowest α values being examined in the brain (Table 1). Generally, the k_d and $t_{1/2}$ for α-TBECH were not significantly different from those for β-TBECH (*t*-test, $p > 0.05$) in individual tissues of zebrafish, indicating diastereomer-dependent accumulation of TBECH in these tissues. As reported in a previous study, the assimilation efficiency of hydrophobic organic chemicals increases with increasing *K*ow at log *K*ow < 7, and then decreases with an increase in log *K*ow values (Fisk et al., 1998). In this study, the log *K*ow values of BTBPE and TBECH were 7.88 and 5.24, respectively, and the assimilation efficiencies were slightly higher for TBECH than those for BTBPE, which is in line with the findings of a previous study (Fisk et al., 1998).

The BMF is a vital parameter determining the integrated outcomes of various processes, encompassing *in vivo* uptake, depuration, and biotransformation. In general, chemicals with log *K*ow values of approximately 5–8 bioaccumulate readily in aquatic organisms (Zheng et al., 2018). In this study, the BMFs of BTBPE and α-/β-TBECH were much less than 1 in all tissues (Table 1), suggesting their low bioaccumulation potential in aquatic organisms. As previously reported in field studies, the bioaccumulation potential of BTBPE and α-/β-TBECH yielded diverse outcomes. BTBPE was found to be magnified in the aquatic food chains (webs) of Taihu Lake (trophic magnification factor, TMF = 2.83) (Zheng et al., 2018), the Bohai Sea (TMF = 2.3) (Liu et al., 2021), and the South China Sea (TMF = 1.91) (Hou et al., 2022). Trophic magnification of TBECH has also been observed in aquatic food chains (webs) in the Bohai Sea (TMF: α-TBECH 1.9, β-TBECH 2.6) (Liu et al., 2021) and South China Sea (TMF = 2.08) (Hou et al., 2022). However,

Table 1
Bioaccumulation parameters of NBFRs in tissues of zebrafish through dietary exposure.

Chemicals	Tissues	Depuration rate (10^{-2}/day) [a]	Half-life (day) [b]	Assimilation efficiency (%) [c]	BMF [d]
BTBPE	Liver	5.64 ± 0.08	12.3 ± 0.17	25.0	0.041
	Brain	3.95 ± 0.13	17.6 ± 0.58	7.78	0.027
	Gonad	4.58 ± 0.14	15.1 ± 0.46	15.9	0.021
	Muscle	3.50 ± 0.22	19.9 ± 1.25	11.6	0.024
α-TBECH	Liver	6.48 ± 0.12	10.7 ± 0.20	34.1	0.049
	Brain	3.89 ± 0.15	17.8 ± 0.69	9.77	0.035
	Gonad	5.34 ± 0.09	13.0 ± 0.22	21.0	0.024
	Muscle	4.26 ± 0.20	16.3 ± 0.77	13.0	0.023
β-TBECH	Liver	6.40 ± 0.16	10.8 ± 0.27	35.0	0.051
	Brain	3.85 ± 0.20	18.0 ± 0.94	10.2	0.037
	Gonad	5.26 ± 0.07	13.2 ± 0.18	22.5	0.025
	Muscle	4.17 ± 0.18	16.6 ± 0.72	13.9	0.025

[a] Depuration rate (k_d) (± standard error): calculated using Eqn. S2 with NBFR concentrations on a lipid weight basis.
[b] Half-life (± standard error): calculated using Eqn. S3.
[c] Assimilation efficiency: calculated using Eqn. S4 on the NBFR concentrations at day 28 of the uptake period (i.e. at the time zero of the depuration period).
[d] Lipid-corrected biomagnification factor (BMF): calculated from Eqn. S5.

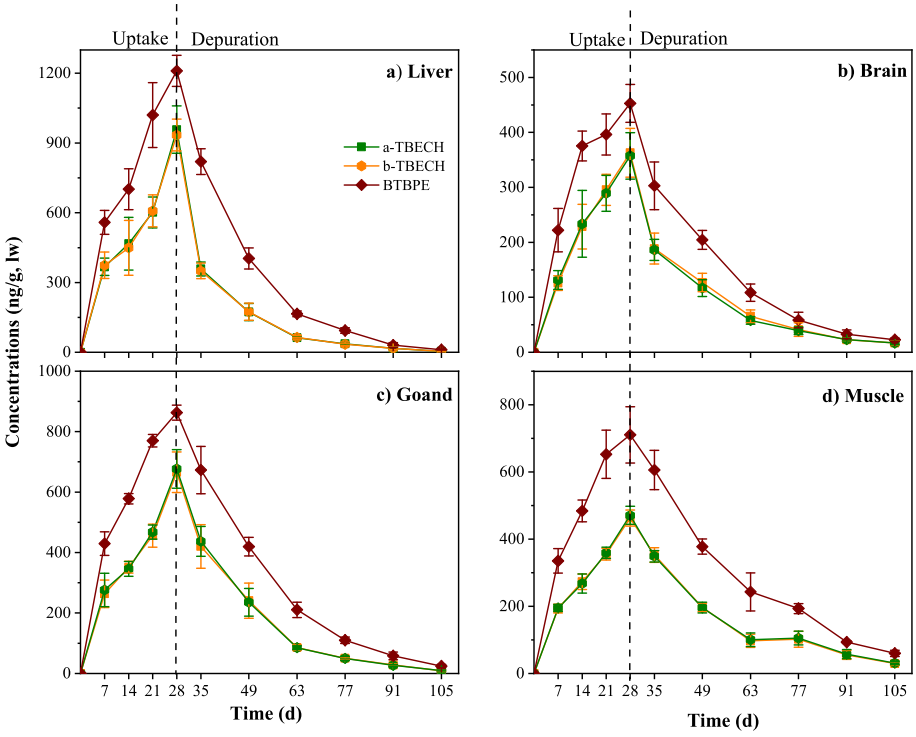

Fig. 1. Uptake and depuration of NBFRs in muscle, liver, gonad, and brain of exposed zebrafish. Error bar indicates ± standard deviation (n = 4 in individual sampling points); lw = lipid weight.

trophic dilution (TMF <1) of BTBPE was observed in the food web of Lake Maggiore (Italy) (TMF = 0.3) (Poma et al., 2014) as well as in a freshwater food web from an electronic waste recycling site in South China (TMF = 0.4) (Wu et al., 2010). Similarly, no significant relationship between α-TBECH concentrations and the trophic levels was found in aquatic food chains (webs) from Taihu Lake, and a relatively low biomagnification potential (TMFs = 0.39) was observed for β-TBECH (Zheng et al., 2018). The variations in the bioaccumulation potential of NBFRs reported in previous studies could be related to the length of the food chains (webs) and the species that constitute them (Hou et al., 2022).

It is should be noted that zebrafish were exclusively exposed to target chemicals through their diet in this study, with careful avoidance of exposure via the aqueous phase. Therefore, the BMF values calculated for BTBPE and α-/β-TBECH in this study cannot be directly compared to the BMF or TMF values reported in field studies mentioned above, where both water and dietary exposure are combined (OECD, 2012). Meanwhile, the levels of BTBPE and α-/β-TBECH did not reach a steady state within the 28-d exposure period in this study; extending the duration of exposure beyond 28 d may potentially result in a more pronounced biomagnification of BTBPE and α-/β-TBECH in zebrafish tissues. The detected NBFR concentrations in the wild organisms generally reflect a prolonged accumulation of BTBPE and α-/β-TBECH, thus a significant biomagnification of these chemicals could be expected in aquatic food webs (Hou et al., 2022; Liu et al., 2021; Zheng et al., 2018).

The biotransformation of NBFRs can also significantly affect their accumulation potential in organisms. Previous studies have indicated that marine fish have slower NBFR biotransformation rates than freshwater fish, resulting in a higher trophic magnification potential of NBFRs in marine food chains (webs) (Hou et al., 2022; Zheng et al., 2018). The observation of BMF <1 for BTBPE and α-/β-TBECH in zebrafish tissues provide new insights for assessment of their ecotoxicology and environmental health risks. The biotransformation of NBFRs in aquatic organisms requires further investigation and is discussed in detail in the following subsections.

3.3. Tissue distribution

As shown in Fig. 1, the levels of BTBPE and α-/β-TBECH were significantly higher in the liver than those in other tissues throughout the exposure period. The liver is richly perfused with blood and serves as the primary organ for deposition of contaminants following their absorption from the gastrointestinal tract. Additionally, it plays a pivotal role in xenobiotic chemical metabolism (Greaves and Letcher, 2014; Zeng et al., 2014), which may account for the liver's high assimilation efficiency and depuration rate of BTBPE and α-/β-TBECH (Table 1). However, poor blood perfusion in the muscle and brain may contribute to lower elimination rates of chemicals in these tissues (Zheng et al., 2014). Moreover, it has been demonstrated that the blood-brain barrier functions as a restrictive mechanism to impede the infiltration of organic chemicals into critical cerebral regions, resulting in the lowest assimilation efficiencies of NBFRs in the zebrafish brain in the present study (Table 1).

The dynamic distribution of BTBPE and α-/β-TBECH was observed among zebrafish tissues. The concentration ratios of liver to other tissues remained relatively stable throughout the exposure period. However, during the depuration period, these ratios exhibited an exponential decline over time (Fig. 2). The concentrations of BTBPE and α-/β-TBECH in the liver can be influenced by enterohepatic circulation and lipophilic contaminant redistribution (Martin et al., 2006), ultimately resulting in the increase in the concentration ratios between the liver and other tissues. Passive diffusion is the primary *in vivo* transportation mode of xenobiotic chemical, wherein the distribution of chemicals in tissues is significantly influenced by the blood perfusion rate and membrane permeability (Esteban and Castaño, 2009). The rates of material exchange between blood and highly vascularized tissues, like the liver, are

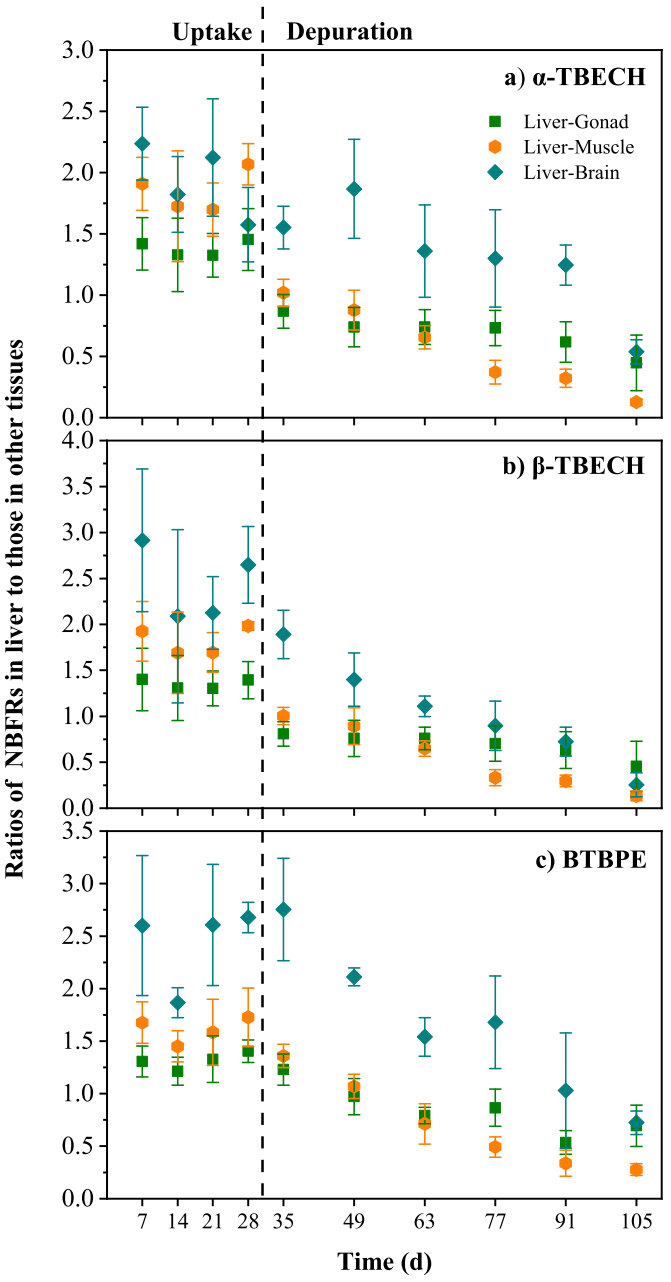

Fig. 2. Concentration ratios of NBFRs in the liver compared to other tissues of zebrafish throughout the experimental period. Error bar indicated ±standard deviation.

generally fast, whereas the rates between blood and muscle or blood and brain tend to be relatively sluggish (Zheng et al., 2014). This is consistent with the result that BTBPE and α-/β-TBECH in the liver have the highest α values compared to other tissues. As the liver is a highly perfused organ that detoxifies toxic substances, NBFRs have been reported to assimilate faster in the liver than in other tissues (Qiao et al., 2023; Shi et al., 2009; Vorkamp et al., 2015).

Furthermore, the relative tissue burdens (RTBs, percent) of BTBPE and α-/β-TBECH were calculated based on their concentrations and the weight in the tissues. As shown in Fig. 3, the RTBs in the liver were relatively high after seven days of exposure, then showed a gradually decreasing trend and tended to stabilize. The RTBs of NBFRs in the muscle were much higher than those in the other tissues during the experiment, and with the extension of the experiment, the load proportion showed an increasing trend (Fig. 3). In the gonads, the RTBs of

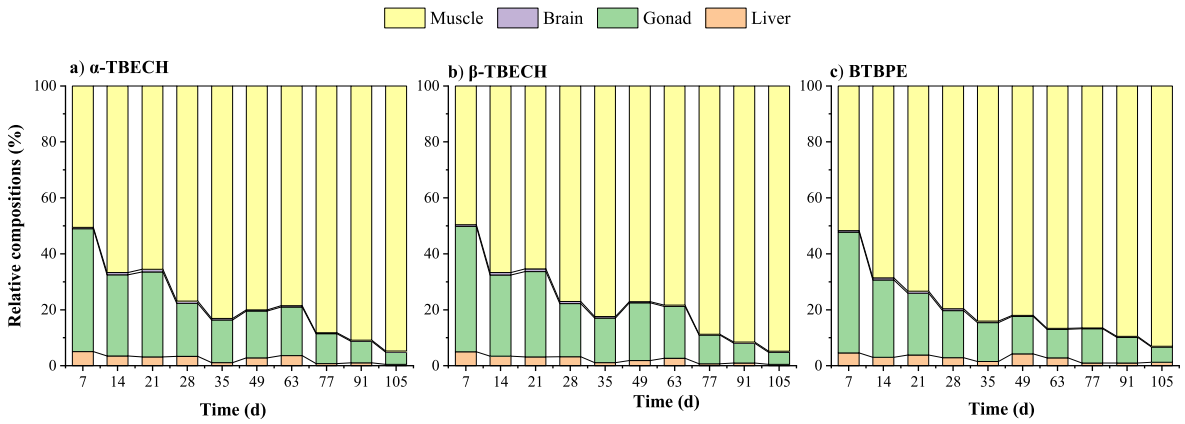

Fig. 3. The relative tissue burdens (%) of NBFRs in zebrafish.

the NBFRs showed a slightly decreasing trend with the extension of the experiment and gradually stabilized at the later stage of clearance (Fig. 3). The main reason for this result may be that sexually mature female zebrafish were used as experimental objects in this study, and the ovary was the second-largest tissue after the muscle. The results of this study indicate that NBFRs have the potential to be enriched in the ovary, which may cause intergenerational transmission and adversely affect offspring.

Additionally, the transport and accumulation of hydrophobic chemicals such as NBFRs within lipid-rich tissues could also contribute significantly to tissue-specific bioaccumulation and distribution in organisms (Hou et al., 2021; Xiong et al., 2019). In this study, the lipid contents in tissues of zebrafish were as follows: gonads (5.92 ± 1.51 %) > muscle (4.66 ± 0.94 %) > liver (3.75 ± 1.39 %) > brain (3.51 ± 0.73 %). As shown in Fig. S3, the wet-weight concentrations of BTBPE and α-/β-TBECH were significantly correlated with the lipid content of zebrafish tissues ($p < 0.001$), revealing the preferential accumulation of BTBPE and α-/β-TBECH in lipid-rich tissues. These results are consistent with those observed in previous studies (Hou et al., 2022; Ruan et al., 2018b; Zheng et al., 2018), in which NBFRs, including BTBPE and TBECH, were significantly positive correlated with the lipid content of aquatic species.

3.4. Enantiomeric selective accumulation of α-/β-TBECH

The physicochemical properties of a pair of chemical enantiomers are identical, and the racemates remain intact (i.e., EF = 0.5)) under achiral interactions, such as abiotic elements (Wong, 2006). The observed deviation of EF = 0.5 suggests the presence of enantioselectivity, which can be attributed to biologically mediated mechanisms like enzymatic biotransformation.

The EFs of α-TBECH and β-TBECH in the administrated food were 0.499 ± 0.005 and 0.499 ± 0.002, respectively, in this study (Fig. 4 A and B). During the uptake period, the EF of α-TBECH gradually increased from 0.596 ± 0.007 to 0.702 ± 0.016 in muscle, from 0.646 ± 0.002 to 0.703 ± 0.005 in gonad, from 0.641 ± 0.009 to 0.757 ± 0.004 in liver, and from 0.619 ± 0.010 to 0.707 ± 0.001 in brain, respectively, which were significantly higher than that in administrated food (Fig. 4A). In the depuration period, the EF of α-TBECH in zebrafish tissues increased with the extending of depuration time (Fig. 4A), which suggested the preferential accumulation of first-eluting (E_1) enantiomer for α-TBECH (E_1-α-TBECH) nd the selective biotransformation of second-eluting (E_2) enantiomer for α-TBECH (E_2-α-TBECH) in zebrafish. Similarly, preferential accumulation of E_1-β-TBECH was observed in zebrafish tissues, exhibiting significantly higher EFs of β-TBECH in zebrafish tissues compared to the technical product (Fig. 4B). Identical enantiomer-selective accumulation trend was observed between α-TBECH and β-TBECH.

The enantiomer-specific accumulation of chiral chemicals is influenced by intricate interactions among processes such as selective absorption, elimination, isomerization, and biotransformation for each individual enantiomer (Li et al., 2016; Yang et al., 2022). The EFs of α- and β-TBECH in zebrafish tissues were higher in the depuration period than those in the uptake period in this study (Fig. 4A and B), providing evidence for the significant role of enantiomer-selective depuration in influencing enantiomer-selective accumulation. However, limited information is available regarding the enantiomeric specificity of TBECH. Selective accumulation of E_1-α-TBECH, E_2-γ-TBECH, and E_1-δ-BECH was observed in mollusk, crustaceans, fish, and cetaceans from the South China Sea; in contrast, no enantioselective accumulation was observed for β-TBECH (Ruan et al., 2018a; Ruan et al., 2018b). Besides, E_2-β-TBECH showed higher microbial degradation rate than E_1-β-TBECH (Ruan et al., 2019), and earthworms were found to selective accumulate E_1-α-TBECH and E_2-γ-TBECH (Yang et al., 2022). These results suggest the enantiomer-selective depuration of TBECH in organisms, which can be attributed to the stereochemical selectivity exhibited by chemicals during biologically mediated processes (Huang et al., 2022; Kania--Korwel and Lehmler, 2016). Therefore, the biotransformation of TBECH in fish requires further investigation.

3.5. Biotransformation of BTBPE and α-/β-TBECH

The potential debrominated transformation products (TPs) of BTBPE and α-/β-TBECH in liver extracts were first screened with GC-ECNI-MS by monitoring m/z 79 and 81. Additionally, ion chromatograms of the control group were compared with those of the exposed group to detect any significant differences. For example, the ion chromatograms of BTBPE and α-/β-TBECH at 28 days of exposure were shown in Figs. S4 and S5. Nine unknown peaks, bromine-containing compounds eluting before BTBPE, and three unknown peaks eluting before α-/β-TBECH were observed (Figs. S4 and S5). These unknown brominated chemicals could be the debromination products of BTBPE and α-/β-TBECH, indicating that the biotransformation of NBFRs does occur in zebrafish.

The potential TPs of BTBPE and α-/β-TBECH were further identified through UPLC-Q-TOF-MS analysis by matching accurate masses (m/z) and possible molecular formulas. Characteristic fragment ions subsequently confirmed their chemical structures (Tables S1 and S2). The extracted ion chromatograms and the accurate mass spectra are given in Figs. S6, S7, S8, and S9, respectively.

Twelve TPs were identified for BTBPE, including a series of ether cleavages, debromination, hydroxylation, and methoxylation reactions (Table S1; Figs. S6 and S7). Metabolic cleavage of the ether linkage of BTBPE resulting in the formation of 2,4,6-tribromophenol (TBP; TP_{BTBPE}-2) and 2,4,6-tribromophenoxyethanol (TBPE; TP_{BTBPE}-5). TBP further underwent debromination, methoxylation, and hydroxylation to form 2,4-dibromophenol (DBP; TP_{BTBPE}-1), 1,3,5-tribromo-methoxy-

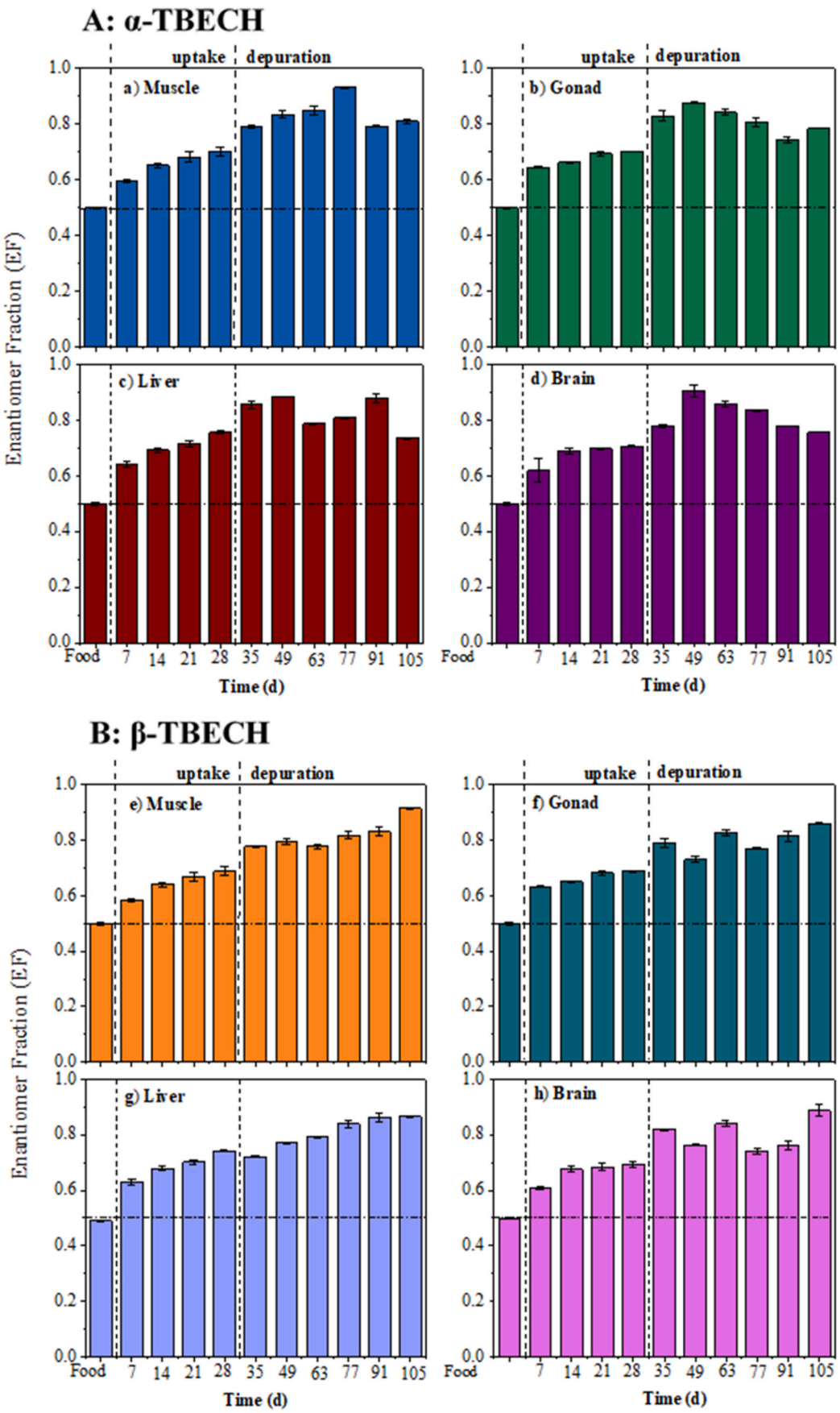

Fig. 4. Enantiomer fractions (EFs) of α-TBECH and β-TBECH in tissues of zebrafish.

benzene (TBMB; TP_{BTBPE}-3), and 1,3,5-tribromo-benzenediol (TBBD; TP_{BTBPE}-4), respectively, while the hydroxylation of TBPE led to the formation of hydroxyl-(2,4,6-tribromophenoxyethanol) (OH-TBPE; TP_{BTBPE}-6) and dihydroxyl-(2,4,6-tribromo-phenoxyethanol) (di–OH–TBPE; TP_{BTBPE}-7).

Aromatic chemicals often oxidize by cytochrome P450s, producing arene oxide as the initial product (Hakk et al., 2004). The cleavage of the BTBPE arene oxide resulted in the formation of a monohydroxylated product (OH-BTBPE; TP_{BTBPE}-12). The accompanied process of arene oxide oxidation and debromination, or the direct debromination of OH-BTBPE produce hydroxyl-(1,3,5-tribromo-2-(2,6-dibromophenyl) benzene) (OH-TBDBPB; TP_{BTBPE}-8). Alternatively, the enzymatic activities of epoxide hydrolase and dihydrodiol dehydrogenase on arene oxide could catalyze the formation of dihydroxyl-(1,3,5-tribromo-2-(2,6-dibromophenyl) benzene) (di–OH–TBDBPB; TP_{BTBPE}-11) isomer I.

Both the aromatic rings of BTBPE underwent cytochrome P450 oxidation. The process of opening the ring and dehalogenation of both arene oxides yield dihydroxyl-bis (dibromophenoxy) ethane (di–OH–BDBPE; TP_{BTBPE}-9), whereas the debromination of only one of the two putative arene oxides resulted in the formation of $TP_{BTB\ PE}$-11, isomer II. Isomers I and II of $TP_{BTB\ PE}$-11 could not be identified in this study because the fragment ions could not distinguish whether the two hydroxyl-groups were on one aromatic ring or different rings (Table S1 and Fig. S7). Finally, the methoxylation of TP_{BTBPE}-9 led to the formation of 3,5-dibromo-4-(2-(2,6-dibromo-methoxyphenoxy) ethoxy) phenol (DBDBMPEP; TP_{BTBPE}-10).

The BTBPE TPs identified in zebrafish livers were similar to those found in rats exposed to BTBPE through their diet (Hakk et al., 2004). TBP has also been identified as a major TP in BTBPE in zebrafish (Qiao et al., 2023) and fathead minnows (de Jourdan et al., 2014). In addition to TBP, hydroxyl metabolites and methoxy TPs of BTBPE have been observed in clams through a water-sediment-clam exposure system (Zhou et al., 2022). These results indicate that the cleavage and debromination of BTBPE are the predominant metabolic transformations *in vivo*. Based on the TPs identified in zebrafish, the BTBPE transformation pathways of BTBPE were proposed in Fig. 5A.

Ten TPs were identified for TBECH, mainly produced through hydroxylation, debromination, and oxidation (Fig. 5B). The hydroxylated TPs included mono-, di-, and tri-hydroxy metabolites, that is, OH-TBECH (TP_{TBECH}-6), di–OH–TBECH (TP_{TBECH}-7), and tri–OH–TBECH (TP_{TBECH}-8). However, α-TBECH and β-TBECH could not be separated through LC analysis in this study. Meanwhile, the precise positions of hydroxyl groups could not be ascertained. The findings of this study are generally in agreement with those obtained from *in vitro* metabolism using rat

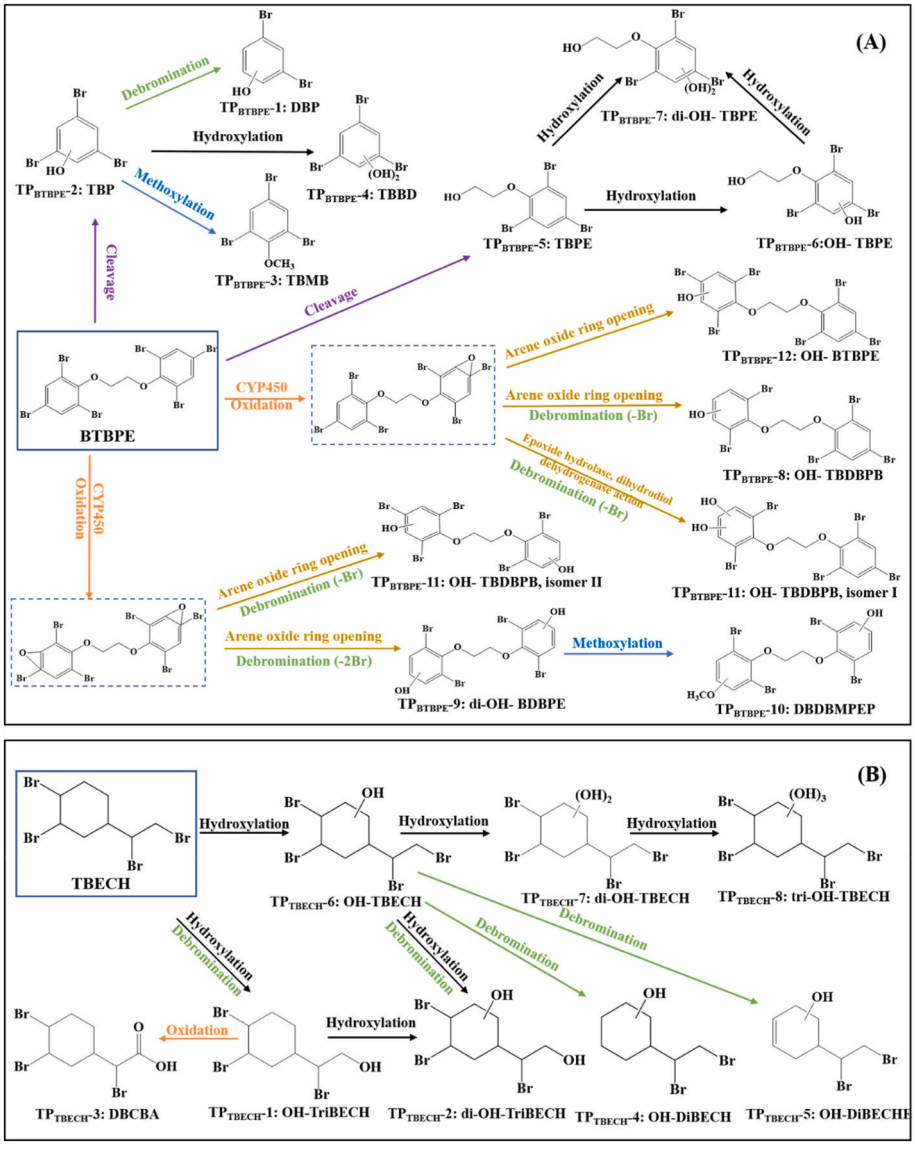

Fig. 5. Proposed biotransformation pathways of (A) BTBPE and (B) TBECH in zebrafish liver.

liver microsomes (RLM) being exposed to the TBECH technical mixture (Chu et al., 2012) and those using human liver microsomes (HLM) following exposure to the α- and β-TBECH isomers (Nguyen et al., 2017).

Additionally, the hydroxylated TPs of debrominated TBECH were identified in the zebrafish liver: mono- and di-hydroxyl-tribromoethyl cyclohexane (TP_{TBECH}-1: OH-TriBECH and TP_{TBECH}-2: di–OH–TriBECH) and hydroxyl-dibromoethylcyclohexane (TP_{TBECH}-4: OH-DiBECH) (Table S2). Although OH-TriBECH and di–OH–TriBECH have been reported in *in vitro* metabolism experiments using HLM (Nguyen et al., 2017) and RLM (Chu et al., 2012), respectively, this is the first study to identify OH-TriBECH, di–OH–TriBECH, and OH-DiBECH *in vivo*. It is reasonable to deduce that OH-TriBECH (TP_{TBECH}-1) can be formed via the debromination of OH-TBECH (TP_{TBECH}-6) and/or directly via the debromination of the parent TBECH, followed by hydroxylation. Further debromination of OH-TBECH (TP_{TBECH}-6) yielded hydroxydibromoethylcyclohexene (TP_{TBECH}-5: OH-DiBECHE) (Table S2). Previous studies have reported similar biotransformation pathways for *in vitro* metabolism of HBCD in rats (Abdallah et al., 2014) and humans (Erratico et al., 2016), in which both hydroxylation and debromination processes were observed. OH-TriBECH (TP_{TBECH}-1) could potentially be formed through the hydroxylation of a tribrominated product of TBECH (i.e., a tribromoethyl cyclohexane derivative or TriBECH), as the debromination of TBECH was detected by GC-MS screening. Although the TriBECH TPs could not be identified in the UPLC-QTOF-MS screening, this hypothesis remains plausible, as triBECH may undergo rapid transformation into its hydroxylated TPs (Nguyen et al., 2017). However, no debromination or hydroxylation TPs of TBECH were detected in earthworms after exposure to a dose of TBECH isomers through soil (Yang et al., 2022), and no debrominated metabolite was observed in the muscle and liver of juvenile rainbow trout following dietary exposure to β-TBECH (Gemmill et al., 2011).

Besides, carboxylated TriBECH, specifically bromo-(1,2-dibromocyclohexyl) acetic acid (TP_{TBECH}-3: DBCBA), is produced through the α-oxidation mechanism. The oxidative reaction initiates at the Cα position, leading to the conversion of the terminal bromomethyl group into an aldehyde, which is subsequently oxidized to form a carboxylic acid (Nguyen et al., 2017). A similar mechanism was reported for the metabolic α-oxidative dehalogenation of structurally similar halogenated chemicals such as tris-2-chloroethyl phosphate (TCEP) (Abdallah et al., 2015). However, the identification of the aldehyde intermediate in this study was hindered due to its susceptibility to rapid oxidation into the corresponding carboxylic acid form (Abdallah et al., 2015). The proposed biotransformation pathways of TBECH based on the TPs identified in zebrafish are shown in Fig. 5B.

Additionally, due to the unavailability of reference standards, the time trends of BTBPE, TBECH, and their major metabolites in zebrafish liver were semi-quantified by assessing the relative peak area (Fig. S10). In the zebrafish liver, the levels of most TPs were similar in magnitude to the parent BTBPE and TBECH, and generally exhibited an increasing trend during the uptake period, followed by a rapid decrease after 7 days of depuration (Fig. S10). This trend was consistent with the findings for BTBPE and TBECH (Fig. 1). However, it is important to note that the contributions were determined based on the relative peak areas of individual TPs, which may significantly deviate from the quantitatively calculated actual contributions using measured concentrations. Furthermore, mass spectrometry analysis did not provide precise positional information regarding additional substituents on the aryl ring of BTBPE and the hexane ring of TBECH. Nonetheless, the results of this study further support that the biotransformation of BTBPE and TBECH significantly decreased their bioaccumulation potential in zebrafish. This is the first study to provide details on the *in vivo* biotansformation of BTBPE and TBECH in zebrafish.

4. Conclusion

In summary, bioaccumulation and biotransformation of BTBPE and TBECH in zebrafish were investigated in the present study. Both BTBPE and TBECH showed low bioaccumulation potential in zebrafish, with BMFs <1 was found in all tissues. The distribution of BTBPE and TBECH was significantly affected by individual tissues' function and fat content. Stereoselective accumulation of TBECH enantiomers was observed in zebrafish tissues, and the inner mechanisms require further investigation. Additionally, the TPs of BTBPE and TBECH were comprehensively screened and identified in the zebrafish liver, and the biotransformation pathways were proposed. Biotransformation significantly affect bioaccumulation potentials of BTBPE and TBECH in zebrafish, and the environmental impacts of their TPs warrant further attention. Over all, we shed new light on the bioaccumulation and biotransformation processes of NBFRs in zebrafish in this study, which provide a scientific basis for accurately assessing their ecological and environmental risks.

CRediT authorship contribution statement

Yu-Yu Wang: Writing – review & editing, Methodology. **Wei-Keng Luo:** Writing – original draft, Investigation. **Song-Xiong Tang:** Writing – review & editing, Investigation. **Jun Xiang:** Writing – review & editing, Investigation. **Yao Dang:** Writing – review & editing, Investigation. **Bin Tang:** Writing – review & editing, Formal analysis, Conceptualization. **Qi-Yuan Lu:** Writing – review & editing, Investigation. **Feng-Shan Cai:** Writing – review & editing, Formal analysis, Data curation. **Ming-Zhong Ren:** Writing – review & editing, Supervision. **Yun-Jiang Yu:** Writing – review & editing, Supervision. **Jing Zheng:** Writing – review & editing, Supervision, Resources, Funding acquisition.

Declaration of competing interest

The authors declare that they have no known competing financial interests or personal relationships that could have appeared to influence the work reported in this paper.

Data availability

Data will be made available on request.

Acknowledgments

This work was financially supported by the National Natural Science Foundation of China (Nos. 42007341, 42377087, 42107467, 42077404, 42222711, and 42007392).

Appendix A. Supplementary data

Supplementary data to this article can be found online at https://doi.org/10.1016/j.envpol.2024.123460.

References

Abdallah, M.A., Uchea, C., Chipman, J.K., Harrad, S., 2014. Enantioselective biotransformation of hexabromocyclododecane by in vitro rat and trout hepatic subcellular fractions. Environ. Sci. Technol. 48, 2732–2740.

Abdallah, M.A., Zhang, J., Pawar, G., Viant, M.R., Chipman, J.K., D'Silva, K., Bromirski, M., Harrad, S., 2015. High-resolution mass spectrometry provides novel insights into products of human metabolism of organophosphate and brominated flame retardants. Anal. Bioanal. Chem. 407, 1871–1883.

Arnot, J.A., Quinn, C.L., 2015. Development and evaluation of a database of dietary bioaccumulation test data for organic chemicals in fish. Environ. Sci. Technol. 49, 4783–4796.

Baduel, C., Lai, F.Y., van Nuijs, A.L.N., Covaci, A., 2019. Suspect and nontargeted strategies to investigate in vitro human biotransformation products of emerging environmental contaminants: the benzotriazoles. Environ. Sci. Technol. 53, 10462–10469.

Bu, Q., Wu, D., Xia, J., Wu, M., Liu, X., Cao, Z., Yu, G., 2019. Polybrominated diphenyl ethers and novel brominated flame retardants in indoor dust of different microenvironments in Beijing, China. Environ. Int. 122, 159–167.

Cao, Z., Zhao, L., Meng, X., Liu, X., Wu, P., Fan, X., Wang, S., Jie, J., Miao, Z., Xu, X., Shen, M., Bu, Q., 2018. Amplification effect of haze on human exposure to

halogenated flame retardants in atmospheric particulate matter and the corresponding mechanism. J. Hazard Mater. 359, 491–499.
Chen, T., Yu, D., Yang, L., Sui, S., Lv, S., Bai, Y., Sun, W., Wang, Y., Chen, L., Sun, Z., Tian, L., Wang, D., Niu, P., Shi, Z., 2019. Thyroid function and decabromodiphenyl ethane (DBDPE) exposure in Chinese adults from a DBDPE manufacturing area. Environ. Int. 133, 105179.
Chu, S., Gauthier, L.T., Letcher, R.J., 2012. Alpha and beta isomers of tetrabromoethylcyclohexane (TBECH) flame retardant: depletion and metabolite formation in vitro using a model rat microsomal assay. Environ. Sci. Technol. 46, 10263–10270.
de Jourdan, B.P., Hanson, M.L., Muir, D.C., Solomon, K.R., 2014. Fathead minnow (Pimephales promelas Rafinesque) exposure to three novel brominated flame retardants in outdoor mesocosms: bioaccumulation and biotransformation. Environ. Toxicol. Chem. 33, 1148–1155.
Eljarrat, E., Guerra, P., Barceló, D., 2008. Enantiomeric determination of chiral persistent organic pollutants and their metabolites. TrAC Trend. Anal. Chem. 27, 847–861.
Erratico, C., Zheng, X., van den Eede, N., Tomy, G., Covaci, A., 2016. Stereoselective metabolism of alpha-, beta-, and gamma-hexabromocyclododecanes (HBCDs) by human liver microsomes and CYP3A4. Environ. Sci. Technol. 50, 8263–8273.
Esteban, M., Castaño, A., 2009. Non-invasive matrices in human biomonitoring: a review. Environ. Int. 35, 438–449.
Fisk, A.T., Norstrom, R.J., Cymbalisty, C.D., Muir, D.C.G., 1998. Dietary accumulation and depuration of hydrophobic organochlorines: bioaccumulation parameters and their relationship with the octanol/water partition coefficient. Environ. Toxicol. Chem. 17, 951–961.
Gemmill, B., Pleskach, K., Peters, L., Palace, V., Wautier, K., Park, B., Darling, C., Rosenberg, B., McCrindle, R., Tomy, G.T., 2011. Toxicokinetics of tetrabromoethylcyclohexane (TBECH) in juvenile brown trout (Salmo trutta) and effects on plasma sex hormones. Aquat. Toxicol. 101, 309–317.
Greaves, A.K., Letcher, R.J., 2014. Comparative body compartment composition and in ovo transfer of organophosphate flame retardants in North American Great Lakes herring gulls. Environ. Sci. Technol. 48, 7942–7950.
Hakk, H., Larsen, G., Bowers, J., 2004. Metabolism, tissue disposition, and excretion of 1,2-bis(2,4,6-tribromophenoxy)ethane (BTBPE) in male Sprague-Dawley rats. Chemosphere 54, 1367–1374.
Harner, T., Wiberg, K., Norstrom, R., 2000. Enantiomer fractions are preferred to enantiomer ratios for describing chiral signatures in environmental analysis. Environ. Sci. Technol. 34, 218–220.
Hou, R., Huang, Q., Pan, Y., Lin, L., Liu, S., Li, H., Xu, X., 2022. Novel brominated flame retardants (NBFRs) in a tropical marine food web from the South China Sea: the influence of hydrophobicity and biotransformation on structure-related trophodynamics. Environ. Sci. Technol. 56, 3147–3158.
Hou, R., Lin, L., Li, H., Liu, S., Xu, X., Xu, Y., Jin, X., Yuan, Y., Wang, Z., 2021. Occurrence, bioaccumulation, fate, and risk assessment of novel brominated flame retardants (NBFRs) in aquatic environments - a critical review. Water Res. 198, 117168.
Huang, H., Guo, B., Wang, D., Kang, Y., Cao, D., Geng, F., Rao, Z., Lv, J., Wen, B., 2022. Bioaccumulation and biotransformation of tetrabromoethylcyclohexane (TBECH) in maize (Zea mays L.): stereoselective driving roles of plant biomacromolecules. J. Hazard Mater. 424, 127610.
Kania-Korwel, I., Lehmler, H.J., 2016. Chiral polychlorinated biphenyls: absorption, metabolism and excretion–a review. Environ. Sci. Pollut. Res. Int. 23, 2042–2057.
Kurt-Karakus, P.B., Muir, D.C.G., de Jourdan, B., Teixeira, C., Epp Martindale, J., Embers, H., Wang, X., Keir, M., Backus, S., 2019. Bioaccumulation of selected halogenated organic flame retardants in Lake Ontario. Environ. Toxicol. Chem. 38, 1198–1210.
Li, B., Wang, K., Ma, L.X., Sun, S.J., Jia, L.R., Yuan, A.N., Shen, J.M., Qi, H., Zhang, A.P., 2018. Deca-BDE and alternative halogenated flame retardants in a wastewater treatment plant in Harbin (2009-2016): occurrence, temporal trends, seasonal variation, and fate. Sci. Total Environ. 625, 1156–1163.
Li, B., Yao, T., Sun, H., Zhang, Y., Yang, J., 2016. Diastereomer- and enantiomer-specific accumulation, depuration, bioisomerization, and metabolism of hexabromocyclododecanes (HBCDs) in two ecologically different species of earthworms. Sci. Total Environ. 542, 427–434.
Li, X., Dong, S., Wang, R., Wang, P., Ruan, Z., Sun, X., Rao, Q., Liu, Z., Su, X., 2019. Novel brominated flame retardant (NBFR) concentrations and spatial distributions in global fishmeal. Ecotoxicol. Environ. Saf. 170, 306–313.
Ling, S., Lu, C., Peng, C., Zhang, W., Lin, K., Zhou, B., 2021. Characteristics of legacy and novel brominated flame retardants in water and sediment surrounding two e-waste dismantling regions in Taizhou, eastern China. Sci. Total Environ. 794, 148744.
Liu, Y., Cui, S., Ma, Y., Jiang, Q., Zhao, X., Cheng, Q., Guo, L., Jia, H., Lin, L., 2021. Brominated flame retardants (BFRs) in marine food webs from Bohai Sea, China. Sci. Total Environ. 772, 145036.
Marteinson, S.C., Palace, V., Letcher, R.J., Fernie, K.J., 2017. Disruption of thyroxine and sex hormones by 1,2-dibromo-4-(1,2-dibromoethyl)cyclohexane (DBE-DBCH) in American kestrels (Falco sparverius) and associations with reproductive and behavioral changes. Environ. Res. 154, 389–397.
Martin, P.A., Mayne, G.J., Bursian, S., Palace, V., Kannan, K., 2006. Changes in thyroid and vitamin A status in mink fed polyhalogenated-aromatic-hydrocarbon-contaminated carp from the Saginaw River, Michigan, USA. Environ. Res. 101, 53–67.
McGrath, T.J., Ball, A.S., Clarke, B.O., 2017. Critical review of soil contamination by polybrominated diphenyl ethers (PBDEs) and novel brominated flame retardants (NBFRs); concentrations, sources and congener profiles. Environ. Pollut. 230, 741–757.
Nguyen, K.H., Abou-Elwafa Abdallah, M., Moehring, T., Harrad, S., 2017. Biotransformation of the flame retardant 1,2-Dibromo-4-(1,2-dibromoethyl)cyclohexane (TBECH) in vitro by human liver microsomes. Environ. Sci. Technol. 51, 10511–10518.
OECD, 2012. Bloaccumulation in Fish: Aqueous and Dietary Exposure. Test Guideline No.305 . Guidelines for the Testing of Chemicals.
Peng, H., Wan, Y., Zhang, K., Sun, J., Hu, J., 2014. Trophic transfer of dechloranes in the marine food web of Liaodong Bay, north China. Environ. Sci. Technol. 48, 5458–5466.
Poma, G., Volta, P., Roscioli, C., Bettinetti, R., Guzzella, L., 2014. Concentrations and trophic interactions of novel brominated flame retardants, HBCD, and PBDEs in zooplankton and fish from Lake Maggiore (Northern Italy). Sci. Total Environ. 481, 401–408.
Qiao, Z., Wang, Y., Lu, C., Ling, S., Zhou, S., Fu, M., Luo, K., Peng, C., Zhang, W., Zhou, B., 2023. Environmental fate of five brominated flame retardants co-exposure in a water-sediment-zebrafish microcosm system: enrichment, removal, and metabolism mechanisms. J. Clean. Prod. 387, 135916.
Ruan, Y., Lam, J.C.W., Zhang, X., Lam, P.K.S., 2018a. Temporal changes and stereoisomeric compositions of 1,2,5,6,9,10-hexabromocyclododecane and 1,2-Dibromo-4-(1,2-dibromoethyl)cyclohexane in marine mammals from the South China Sea. Environ. Sci. Technol. 52, 2517–2526.
Ruan, Y., Zhang, K., Lam, J.C.W., Wu, R., Lam, P.K.S., 2019. Stereoisomer-specific occurrence, distribution, and fate of chiral brominated flame retardants in different wastewater treatment systems in Hong Kong. J. Hazard Mater. 374, 211–218.
Ruan, Y., Zhang, X., Qiu, J.W., Leung, K.M.Y., Lam, J.C.W., Lam, P.K.S., 2018b. Stereoisomer-specific trophodynamics of the chiral brominated flame retardants HBCD and TBECH in a marine food web, with implications for human exposure. Environ. Sci. Technol. 52, 8183–8193.
Shi, J., Wang, X., Chen, L., Deng, H., Zhang, M., 2021. HBCD, TBECH, and BTBPE exhibit cytotoxic effects in human vascular endothelial cells by regulating mitochondria function and ROS production. Environ. Toxicol. 36, 1674–1682.
Shi, T., Chen, S.J., Luo, X.J., Zhang, X.L., Tang, C.M., Luo, Y., Ma, Y.J., Wu, J.P., Peng, X. Z., Mai, B.X., 2009. Occurrence of brominated flame retardants other than polybrominated diphenyl ethers in environmental and biota samples from southern China. Chemosphere 74, 910–916.
Stojak, B.L., van Ginkel, R.A., Ivanco, T.L., Tomy, G.T., Fry, W.M., 2019. Acute beta-tetrabromoethylcyclohexane (beta-TBECH) treatment inhibits the electrical activity of rat Purkinje neurons. Chemosphere 231, 301–307.
Tang, B., Luo, X.J., Huang, C.C., Ren, Z.H., Zeng, Y.H., Mai, B.X., 2018. Characterizing the influence of metabolism on the halogenated organic contaminant biomagnification in two artificial food chains using compound- and enantiomer-specific stable carbon isotope analysis. Environ. Sci. Technol. 52, 10359–10368.
Tang, B., Xiong, S.M., Zheng, J., Wang, M.H., Cai, F.S., Luo, W.K., Xu, R.F., Yu, Y.J., 2021. Analysis of polybrominated diphenyl ethers, hexabromocyclododecanes, and legacy and emerging phosphorus flame retardants in human hair. Chemosphere 262, 127807.
Tomy, G.T., Palace, V.P., Pleskach, K., Ismail, N., Oswald, T., Danell, R., Wautier, K., Evans, B., 2007. Dietary exposure of juvenile rainbow trout (Oncorhynchus mykiss) to 1,2-bis(2,4,6-tribromophenoxy)ethane: bioaccumulation parameters, biochemical effects, and metabolism. Environ. Sci. Technol. 41, 4913–4918.
Vorkamp, K., Bossi, R., Riget, F.F., Skov, H., Sonne, C., Dietz, R., 2015. Novel brominated flame retardants and dechlorane plus in Greenland air and biota. Environ. Pollut. 196, 284–291.
Wang, G., Du, Z., Chen, H., Su, Y., Gao, S., Mao, L., 2016. Tissue-specific accumulation, depuration, and transformation of triphenyl phosphate (TPHP) in adult zebrafish (Danio rerio). Environ. Sci. Technol. 50, 13555–13564.
Wang, X., Ling, S., Guan, K., Luo, X., Chen, L., Han, J., Zhang, W., Mai, B., Zhou, B., 2019. Bioconcentration, biotransformation, and thyroid endocrine disruption of decabromodiphenyl ethane (dbdpe), A novel brominated flame retardant, in zebrafish larvae. Environ. Sci. Technol. 53, 8437–8446.
Wang, Z., Jia, H., Jiang, Y., Cui, S., Li, Y.F., 2023. Bioaccumulation of novel brominated flame retardants in crucian carp (Carassius auratus): implications for electronic waste recycling area monitoring. Environ. Res. 239, 117412.
Wong, C.S., 2006. Environmental fate processes and biochemical transformations of chiral emerging organic pollutants. Anal. Bioanal. Chem. 386, 544–558.
Wu, J.P., Guan, Y.T., Zhang, Y., Luo, X.J., Zhi, H., Chen, S.J., Mai, B.X., 2010. Trophodynamics of hexabromocyclododecanes and several other non-PBDE brominated flame retardants in a freshwater food web. Environ. Sci. Technol. 44, 5490–5495.
Xiong, P., Yan, X., Zhu, Q., Qu, G., Shi, J., Liao, C., Jiang, G., 2019. A review of environmental occurrence, fate, and toxicity of novel brominated flame retardants. Environ. Sci. Technol. 53, 13551–13569.
Xiong, Q., Liu, Y.S., Hu, L.X., Shi, Z.Q., Cai, W.W., He, L.Y., Ying, G.G., 2020. Co-metabolism of sulfamethoxazole by a freshwater microalga Chlorella pyrenoidosa. Water Res. 175, 115656.
Yang, E., Wen, B., Zhang, Z., Huang, H., Zhang, S., 2022. Diastereomer- and enantiomer-selective accumulation and depuration of 1,2-dibromo-4-(1,2-dibromoethyl) cyclohexanes (DBE-DBCHs) and 1,2,5,6-tetrabromocyclooctanes (TBCOs) in earthworms (Eisenia fetida). Sci. Total Environ. 826, 154145.
Zeng, Y.H., Luo, X.J., Tang, B., Zheng, X.B., Mai, B.X., 2014. Gastrointestinal absorption, dynamic tissue-specific accumulation, and isomer composition of dechlorane plus and related analogs in common carp by dietary exposure. Ecotoxicol. Environ. Saf. 100, 32–38.
Zheng, G., Wan, Y., Shi, S., Zhao, H., Gao, S., Zhang, S., An, L., Zhang, Z., 2018. Trophodynamics of emerging brominated flame retardants in the aquatic food web

of Lake Taihu: relationship with organism metabolism across trophic levels. Environ. Sci. Technol. 52, 4632–4640.
Zheng, X.-B., Luo, X.-J., Zeng, Y.-H., Wu, J.-P., Mai, B.-X., 2014. Sources, gastrointestinal absorption and stereo-selective and tissue-specific accumulation of Dechlorane Plus (DP) in chicken. Chemosphere 114, 241–246.
Zhou, S., Fu, M., Luo, K., Qiao, Z., Peng, C., Zhang, W., Lei, J., Ling, S., Zhou, B., 2022. Fate and toxicity of legacy and novel brominated flame retardants in a sediment-water-clam system: bioaccumulation, elimination, biotransformation and structural damage. Sci. Total Environ. 840, 156634.
Zuiderveen, E.A.R., Slootweg, J.C., Boer, J.D., 2020. Novel brominated flame retardants - a review of their occurrence in indoor air, dust, consumer goods and food. Chemosphere 255, 126816.